საქართველოს მეცნიერებათა ეროვნული აკადემიის მოამბე, ტ. 13, №4, 2019
BULLETIN OF THE GEORGIAN NATIONAL ACADEMY OF SCIENCES, vol. 13, no. 4, 2019

Biophysics

Revealing a Nonergodic Mechanistic Pattern for Electron Exchange between Azurin and Electrodes Coated by Nano-Films under the Glassy Environmental Conditions

Tinatin Dolidze[*], Rudi van Eldik[**], Dimitri Khoshtariya[*,§]

[*] *Ivane Beritashvili Center of Experimental Biomedicine, Tbilisi, Georgia*
[**] *Friedrich-Alexander University of Erlangen-Nuremberg, Germany*
[§] *Ivane Javakhishvili Tbilisi State University, Tbilisi, Georgia*

(Presented by Academy Member David Mikeladze)

ABSTRACT. Fast-scan protein-film voltammetry was applied to explore interfacial biomimetic electron exchange under the environmental glass forming conditions. Gold electrodes were coated with 1-pentanethiol SAM–azurin (Az, blue cupredoxin) assemblies and placed in contact with a water-doped and buffered protic ionic melts of choline dihydrogen phosphate ([ch][dhp]), served as electrolyte media, allowing for a necessary cell conductivity under the virtually solid, semi-solid and liquid electrolyte conditions over 273–353 K, within which the electron exchange rate was studied as a function of the water amount and temperature. Exposure of the Az films to the semi-solid electrolyte greatly affected the protein's conformational dynamics, hence the ET rate, via the mechanism occurring in the extra complicated dynamically-controlled regime. Results are compared to the earlier studies on the reference system with a conventional electrolyte, allowing for the disclosure of mutually-entangled mechanistic motifs. Under the "standard" condition (with no [ch][dhp] added), the Az biomolecule may reside in an apparently ergodic state, whereas upon adding of [ch][dhp] to allow water content ranging between 6 to 15 waters per [ch][dhp], system displays anomalous temperature dependences, suggesting that the reactive system crosses a broad, well-manifested nonergodic zone which arises from the continuous interplay (freezing/unfreezing) of ET-coupled highly cooperative conformational modes of the Az protein, inherently linked to the electrolyte's slowest collective relaxation(s). Above this [ch][dhp] concentration, allowing the water content between 1.65 to 3.7 waters per ion pair, the system returns to a series of new, quasi-ergodic states, with each displaying virtually linear Arrhenius patterns yet with distinct parameters. *© 2019 Bull. Georg. Natl. Acad. Sci.*

Key words: redox protein, electron exchange, interphase, self assembly, nonergodicity

The vitally important biochemical processes in biological organisms (living cells and tissues) take place in rather crowded environments forming concentrated solutions of versatile natural buffer components and different kind of regulatory or substrate-like organic molecules [1-3]. In many

cases these environments are the extremely viscous media and of essentially glass forming (factually, of the semi-solid) rather than simple liquid-like texture [4,5]. Therefore, the semi-solid hybrid (organic/inorganic) blends may provide a more realistic mimic of the environment in a cell or biological membrane than does a simple aqueous electrolyte [6,7]. Consequently, kinetic studies of redox processes within such the assemblies/blends are highly relevant and may improve our understanding of electron transfer in biological organisms and structures. Semisolid conditions that normally offer notable protein preservation also raise some novel challenging mechanistic questions. However, systematic mechanistic studies of interfacial biological ET in glassy media by the standard voltammetry methods have been limited because of the poor solution conductivity of the semi-rigid environment and/or the extra-demanding cryogenic requirements. Fortunately, the protic ionic substance, choline dihydrogen phosphate ([ch][dhp]), have been reported to possess significant ionic (particularly protic) conductance and remarkable bio-compatibility [8-10], involvement of which, along with the enhancement of the stability and robustness of electroactive Au–SAM–protein assemblies, allows, on the one hand, to approach a solid-like (glassy) state under nearly ambient experimental conditions and, on the other hand, to warrant settings for obtaining the artifact-free, hence, fully reliable voltammetry data.

In our earlier work (see papers [11-13]) we demonstrated the ability of fast-scan cyclic voltammetry to be a very powerful biophysical method to study intrinsic physical mechanisms of redox-active proteins. In this work the Au–SAM–Az assembly (consisting of the alkanethiol SAM with methylene carbon numbers of 4, and Az, azurin, blue cupredoxin) was placed in contact with a buffered protic ionic melt, [ch][dhp], containing 2 to 15 water molecules per [ch][dhp] ion pair (content of the ionic component varied from 50 to 90% w/w), and the ET was studied as a function of temperature (273–353 K) by fast-scan cyclic voltammetry, in order to obtain new insights regarding the novel mechanistic aspects for the electron exchange occurring within the semi-solid and almost solid, that is, ultraviscouse (glass forming) environment.

Materials and Methods

Highly purified P. aeruginosa azurin was purchased from Sigma and was used without further purification. The starting material for the buffer doped ionic melt, choline dihydrogen phosphate ([ch][dhp]) was purchased from Ionic Liquids Technologies (Iolitech, GmbH) and was used as received. The 1-pentanethiol, highest purity commercially available (Acros) was used as received. The buffer components, ultrapure 5 M ammonium acetate and HClO4 (70%) were from Fluka. The Az films were prepared according to published procedures. All the PIM blends were adjusted to have pH 4.6 [12].

The Az film voltammetry was carried out with an Autolab Electrochemical Analyzer GSTAT 30. The electrochemical cell has been described elsewhere [11-13]; GPES software was used for the primary data analysis and the ‘‘post-measurement’’ Ohmic potential drop corrections for the experimental CV response The conductivity of all aqueous [ch][dhp] blends (work solutions) was checked by standard instrumentation. It was found that conductivity of all solutions was high enough that the iR drop correction had no significant impact on the voltammetric data. Nevertheless, the post-measurement software-aided corrections were made [11-13]; hence the results reported in this paper are essentially free of Ohmic potential drop errors.

Results and Discussion

Fig. 1, panel (A) shows chemical composition of ([ch][dhp]), whereas Fig. 1, panel (B) depicts typical cyclic voltammograms for the azurin electron exchange at Au/SAM junctions Az at a

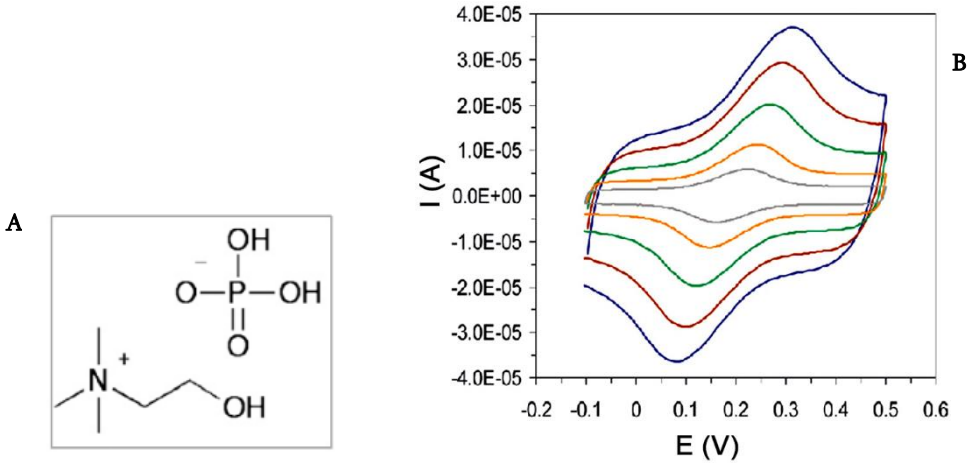

Fig. 1. (A) Chemical composition of choline dihydrogen phosphate ([ch][dhp]). (B) CV records for the electron exchange of Az at a 1-pentanethiol (n = 4) SAM coated Au electrode placed in a70% (w/w) [ch][dhp] solution (pH 4.6, at 20^0C); potential scan rates: 10, 20, 40, 60 and 80 V s^{-1} (the peak intensity increase).

1-pentanethiol (n=4) SAM coated Au electrode placed in a 70% (w/w) [ch][dhp] solution (pH 4.6, at 20^0C); potential scan rates: 10, 20, 40, 60 and 80 V s^{-1}. Very accurate and stable CV curves obtained throughout and application of standard data-processing methodology that is based on the extended Marcus theory [11-14] allowed us to determine standard kinetic constants and respective activation parameters for the Mb electron transfer/exchange (ET).

Fig. 2, panel (A) displays evolution of conductivity for the buffered aqueous [ch][dhp] blends (pH 4.6) as a function of the molar fraction of the [ch][dhp] component, denoted as "X", at 20^0C. Data for a pure solid [ch][dhp] (amounting to ca. 10–5 S/m) are taken from Ref. [9]. Fig. 2, panel (B) shows an Arrhenius-type plot for the conductivity temperature dependence of a 90% (w/w) buffered aqueous [ch][dhp] blend (pH 4.6). Blue curve depicts the polynomial fit to the

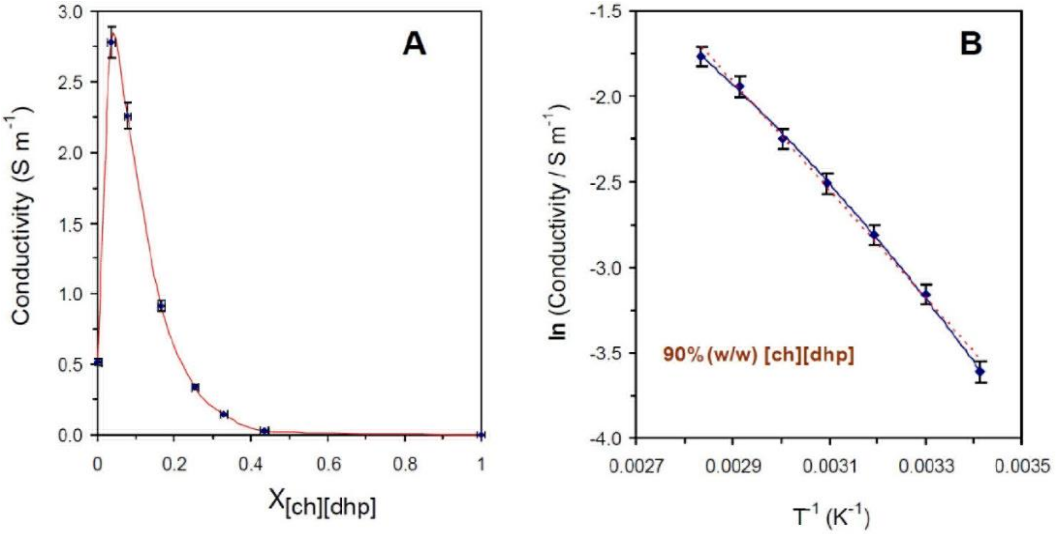

Fig. 2. (A) Evolution of the conductivity for the buffered aqueous [ch][dhp] blends (pH 4.6) as a function of the molar fraction of the [ch][dhp] component, at 20^0C. Data for a pure solid [ch][dhp] are taken from Ref. [9]. (B) Arrhenius-type plot for the conductivity temperature dependence of a 90% (w/w) buffered aqueous [ch][dhp] blend (pH 4.6). Blue curve – the polynomial fit; dashed red line – the linear fit.

experimental poins, whereas the dashed red line – the linear fit. From these results one may see that the electrolyte conductivity within the whole concentration range of the ionic component, [ch][dhp], is sufficient to warrant with an excess the artifact-free determination of electron exchange rate constants (vide supra).

Unlike the case of an aqueous electrolyte [12] (considered here as a standard one) and despite the overall increased stability of the assemblies with regard to the temperature variation (vide supra), the rate constant data in Fig. 3, panels (A) and (B), show a very peculiar behavior. In particular, for cases with moderate additive concentrations around 50-70% w/w (matching the water amount of ca. 15.0 to 6.25 waters per [ch][dhp] ion pair), the rate constants display hysteresis with the temperature cycling, and dramatically variable slopes of plots for the rate constant, $\ln(k^0)$ vs. T. This behavior was observed for multiple different samples and scans. The linearity, reversibility, and reproducibility were restored starting with the case of 80% [ch][dhp] and above matching ca. 3.70, 2.55 and 1.65 waters per ion pair). Specifically, Fig. 3, panel (A) depicts Arrhenius plots for ET rate constants of Az immobilized at SAM (n = 4) coated Au electrodes, placed in a water-doped and buffered (pH 4.6) protic ionic melt containing 0 (ref. [12]), 80 (blue), 85 and 90% (w/w) [ch][dhp] (from top to bottom). The data for 50 and 70% mixtures fall with the so called "Nonergodic Zone" (vide infra) indicated by the stretched ellipsoid in yellow color, display "anomalous" Arrhenius plots, are depicted separately (expanded) in the panel (B) of this Fig.. Fig. 3, panel (B) depicts Arrhenius plots for ET rate constants of Az immobilized at SAM (n=4) coated Au electrodes placed in a water-doped and buffered (pH 4.6) protic ionic melt containing 50% (dashed curves) and 70% (solid curves) ([ch][dhp]) w/w. Open and filled symbols indicate cycles with a temperature increase and decrease, respectively. A linear Arrhenius plot below represents a system with 80% [ch][dhp] (shown in the panel A as well), depicted here for the comparison. Within the [ch][dhp] concentration range of 50 to 70% w/w, systems exhibited a behavior that is typical for the nonergodic pattern [15-20] (vide infra), while above 80%, the quasi-ergodic behavior restored, indicating that some distinguished degrees of freedom that survived freezing, could withstand further increase of the additive concentration, and displayed "normal" Arrhenius patterns.

In earlier work on Au–SAM–Az aqueous electrolyte junctions [12], we showed that the electron transfer mechanism falls within the dynamically-controlled regime for thin SAMs. In this kinetic mechanistic regime, heterogeneous "adiabatic" rate constant, k_A^0, of electron exchange can be presented as [11-14,21,22]:

$$k_A^0 = \frac{1}{\tau_{eff}} \sqrt{\frac{\lambda_0}{\pi^3 RT}} \exp(-\Delta G_a / RT), \qquad (1)$$

where λ_0 is the reorganization free energy of the complex environment (in the sense of Marcus), ΔG_a is the free energy of activation of the exchange process and τ_{eff} is the effective characteristic time related to relaxation processes of the solvent molecules, protein interior, etc. (other symbols attain their traditional meaning). In the approximation of a dielectric continuum and a Debye-type dielectric response, one finds that:

$$\tau_{eff} \approx \tau_L = \left(\frac{\varepsilon_\infty}{\varepsilon_s}\right) \frac{3\eta V_m}{RT}, \qquad (2)$$

where τ_L is the longitudinal relaxation time of the solvent polarization and η is the solvent viscosity. The other parameters are the molar volume V_m, the static dielectric constant ε_s, and the high-frequency dielectric constant ε_∞. For the case of more complex environments, τ_{eff} might be associated with some conformational or molecular rearrangement that is coupled to the electron transfer.

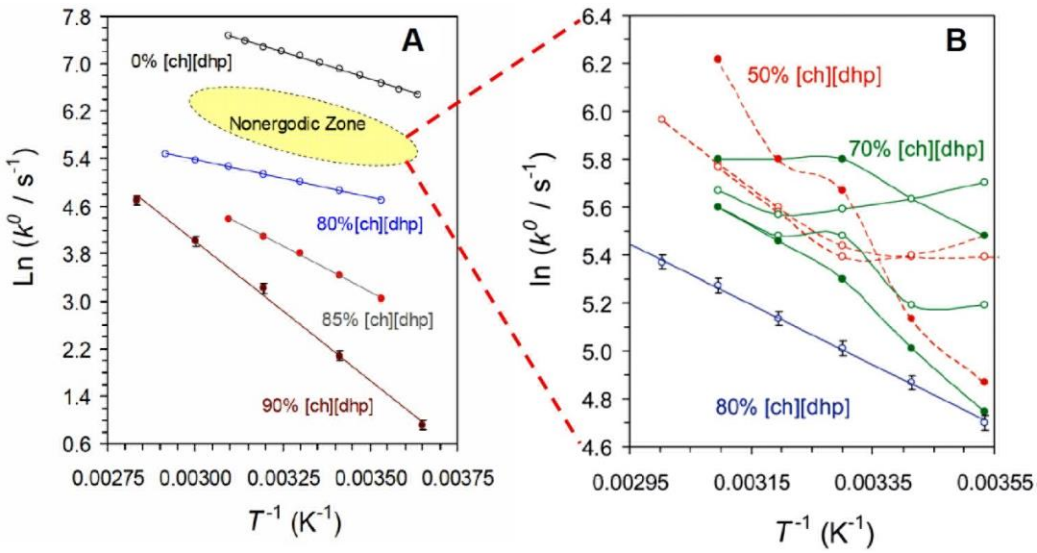

Fig. 3. (A) Arrhenius plots for ET rate constants of Az immobilized at SAM (n = 4) coated Au electrodes, placed in a water-doped and buffered (pH 4.6) protic ionic melt containing 0 (ref. X), 80 (blue), 85 and 90% (w/w) [ch][dhp] (from top to bottom). The data for 50 and 70% mixtures fall with the "Nonergodic Zone" indicated by the stretched ellipse in yellow color, display "anomalous" Arrhenius plots, are depicted separately (expanded) in the panel B of this Fig. **(B)** Arrhenius plots for ET rate constants of Az immobilized at SAM (n = 4) coated Au electrodes placed in a water-doped and buffered (pH 4.6) protic ionic melt containing 50% (dashed curves) and 70% (solid curves) ([ch][dhp]) w/w. Open and filled symbols indicate cycles with a temperature increase and decrease, respectively. A linear Arrhenius plot below represents a system with 80% [ch][dhp] (shown in the panel A as well), depicted here for the comparison.

Within the present research effort, we extended our previous work [12] to examine the same Au/1-pentanethiol (n= 4) SAM/Az junction through the application of a novel experimental design allowing for the unprecedentedly broad variation of a key tuning parameter τ_{eff}, made possible through the changes of solution composition and temperature. These studies clearly indicated that, along the solvent control adiabetic mechanism showing via applicability of equations (1) and (2) (as has been demonstrated before [12]), under certain experimental conditions, the novel kinetic features, such as nonlinear and hysteretic Arrhenius dependencies (predicted as to be typical for the mechanistic pattern of nonergodic environmental impact [15-20]) can be observed and explored systematically. Importantly, nonergodicity (dynamical arrest) and accompanying kinetic effects should be even more well-pronounced when appear in combination with the short-range (dynamically-controlled) ET in glass-forming media, for which the broad spectrum of slowly relaxing degrees of freedom directly determine the rate constant through the pre-exponential term of the rate equation, (1), also (2).

In summary, the sandwich-like nano-assemblies composed of gold-deposited alkanethiol SAMs and on top immobilized films of the redox-active protein azurin, additionally were placed in contact with semi-solid electrolytes, the buffered protic ionic melts of variable doping water content. The fast-scan voltammetry studies of biomimetic ET under the conditions of approaching a glassy state revealed the combined operation of the both, dynamically controlled (adiabatic) and medium's nonergodic response mechanistic patterns. We propose that this kind of interplay should be typical for biomolecular processes proceeding in overcrowded intercellular environments.

The work was supported by Shota Rustaveli National Science foundation of Georgia (SRNSFG), Grant Number: FR 17_570.

ბიოფიზიკა

აზურინსა და ნანო-ფირებით დაფარულ ელექტროდებს შორის ელექტრონების მიმოცვლის არაერგოდიკული მექანიზმის გამოვლინება მინისებრი გარემოს პირობებში

თ. დოლიძე*, რ. ვან ელდიკი**, დ. ხოშტარია*,§

* *ივანე ბერიტაშვილის ექსპერიმენტული ბიომედიცინის ცენტრი, თბილისი, საქართველო*
** *ფრიდრიხ-ალექსანდერის უნივერსიტეტი, ერლანგენ-ნიურნბერგი, გერმანია*
§ *ივანე ჯავახიშვილის თბილისის სახელმწიფო უნივერსიტეტი, თბილისი, საქართველო*

(წარმოდგენილია აკადემიის წევრის დ. მიქელაძის მიერ)

სარეაქციო გარემოს მინისებრი მდგომარეობის პირობებში ელექტრონების მიმოცვლის ბიომიმეტიკური პროცესის შესწავლის მიზნით გამოყენებული იყო სწრაფი სკანირების ვოლტამპერომეტრიის მეთოდი. ჟანგვა-აღდგენითი ფუნქციის მქონე ცილა აზურინი (ლურჯი კუპრედოქსინი) იმობილიზებული იყო ოქროს ელექტროდებზე თვითაწყობილ ალკანთიოლურ (1-პენტანოთიოლის) ფირებზე და, იმავდროულად, კონტაქტში იმყოფებოდა ზებლანტ ელექტროლიტურ ლღობილებთან – წყლის მოლეკულებით და ბუფერის კომპონენტებით შეზავებული ორგანული იონური მარილის, ქოლინ დიჰიდროგენ ფოსფატის, ([ch][dhp]) 50-დან 90%-მდე (წონითი წილის) ხსნარებთან. ეს უზრუნველყოფდა ვოლტამპერომეტრული მეთოდის გამოყენებისთვის აუცილებელ ცილის გარემოს ელექტროგამტარობას ტემპერატურის ფართო დიაპაზონში (273–353 K), რომელიც ფარავს ელექტროლიტური ხსნარის როგორც მყარ, ისე ნახევრად მყარ და თხევად მდგომარეობებს. მოცემული თვისებების გარემოში ცილის მოთავსება საშუალებას იძლევა, რომ შესწავლილ იქნეს ბიომოლეკულის ფუნქციური აქტივობა (კინეტიკა, ენერგეტიკა და ფიზიკური მექანიზმი) მის ბუნებრივ გარემოსთან ბევრად უფრო მიახლოებულ პირობებში განზავებულ წყალხსნარებთან შედარებით. თანამედროვე თეორიული წარმოდგენების და ჩვენი ადრინდელი მონაცემების მიხედვით, აზურინი, მოცემულ ექსპერიმენტულ პირობებში, ფუნქციონირებს ე. წ. „დინამიკური კონტროლის“ რეჟიმში. ახლად მიღებული მონაცემები კი ცხადყოფს, რომ სტანდარტულ პირობებში ([ch][dhp]-ის დანამატებისგან თავისუფალ გარემოში) აზურინი ასევე იმყოფება ე.წ. კვაზი-ერგოდიკულ მდგომარეობაში, რაც გამოიხატება სპეციფიკური კინეტიკური გამოვლინებების არარსებობით. იონური დანამატების პირობებში, როდესაც ერთ [ch][dhp] იონ-წყვილზე მოდის მხოლოდ 6-დან 15-მდე წყლის მოლეკულა, პროცესის არაერგოდიკული ბუნება გამოვლინდება სრულად, როგორც არენიუსის ტემპერატურული დამოკიდებულების ძლიერი არაწრფივი და ჰისტერიზისული ანომალიები. იონური დანამატის კიდევ უფრო მაღალი კონცენტრაციების პირობებში (1,65-დან 3,7-მდე წყლის მოლეკულა ერთ იონურ წყვილზე) კვაზი-ერგოდიკული მდგომარეობა ისევ ხდება შენიღბული, მაგრამ არენიუსის დამოკიდებულების „კლასიკური“ ფორმა ბრუნდება უკვე სხვა ეფექტური პარემეტრების გამოვლინების მეშვეობით. ეს ყველაფერი მიუთითებს აზურინის ბიომოლეკულის არსებითად არაერგოდიკული ბუნების შესახებ, რაც

ზოგადად დამახასიათებელი უნდა იყოს ბიომოლეკულებისთვის და, რომლის გამოვლინება ხდება შესაფერისი ექსპერიმენტული პირობების შერჩევის გზით.

REFERENCES

1. Ellis R.J. (2001) Macromolecular crowding: an important but neglected aspect of the intracellular environment. *Curr. Opinion Struct. Biol.* **11**:114–119.
2. Zhow H.-X., Rivas G., Minton A.P. (2008) Macromolecular crowding and confinement: biochemical, biophysical and potential physiological consequences. *Annual Rev. Biophys.*, **37**:375–397.
3. Mittal S., Chowhan R.K., Singh L.R. (2015) Macromolecular crowding: macromolecules' friend or foe. *Biochim. Biophys. Acta* **1850**:1822–1831.
4. Frauenfelder H. et al. (2009) A unified model of protein dynamics. *Proc. Natl. Acad. Sci. USA* **106**:5129–5134.
5. Jansson H., Bergman R., Swenson J. (2011) Role of solvent for the dynamics and the glass transition of proteins. *J. Phys. Chem. B* **115**:4099–4109.
6. Lee A.G. (2004) How lipids affect the activities of integral membrane proteins. *Biochim. Biophys. Acta* **1666**:62–87.
7. Bondar A.-N., WhiteS.H. (2004) Hydrogen bond dynamics in membrane protein function. *Biochim. Biophys. Acta* **1818**:942–950.
8. Belieres J.-P., Angell C.A. (2007) Protic ionic liquids: preparation, characterization and proton free energy level representation. *J. Phys. Chem. B* **111**:4926–4937.
9. Rana U.A. et al. (2010) Proton transport in choline dihydrogen phosphate/H_3PO_4 mixtures. *Phys. Chem. Chem. Phys.* **12**:11291–11298.
10. Fujita K., Ohno H. (2010) Enzymatic activity and thermal stability of metallo proteins in hydrated ionic liquids. *Biopolymers* **93**:1093–1099.
11. Khoshtariya D.E. et al. (2006) Kinetic, thermodynamic, and mechanistic patterns for free (unbound) cytochrome c at Au/SAM junctions: impact of electronic coupling, hydrostatic pressure, and stabilizing/denaturing additives. *Chemistry - A European J.* **12**:7041–7056.
12. Khoshtariya D.E. et al. (2010) Fundamental signatures of short and long-range electron transfer for the blue copper protein azurin at Au/SAM junctions. *Proc. Natl. Acad. Sci. USA* **107**:2757–2762.
13. Khoshtariya D.E. et al. (2014) Long-range electron transfer with myoglobin immobilized at Au/Mixed-SAM junctions: mechanistic impact of the strong protein confinement. *J. Phys. Chem. B* **118**:692–706.
14. Weber K., Hockett L., Creager S. (1997) Long-range electronic coupling between ferrocene and gold in alkanethiolate-based monolayers on electrodes. *J. Phys. Chem. B* **101**:8286–8291.
15. Palmer R.G. (1982) Broken ergodicity. *Adv. Phys.* **31**:669–735.
16. Mauro J.C., Gupta P.K., Loucks R.J. (2007) Continuously broken ergodicity. *J. Chem. Phys.* **126**:184511 (11p.).
17. Mallamace F. et al. (2011) The role of the dynamic crossover temperature and the arrest in glass-forming fluids. *Eur. Phys. J. E* **34**;94 (94p).
18. Lebard D.N., Matyushov D.V. (2010) Protein-water electrostatics and principles of bioenergetics. *Phys. Chem. Chem. Phys.***12**:15335–15348.
19. Matyushov D.V. (2011) Nanosecond stokes shift dynamics, dynamical transition, and gigantic reorganization energy of hydrated heme proteins. *J. Phys. Chem. B*, **115**:10715–10724.
20. Matyushov, D.V. (2013) Protein electron transfer: dynamics and statistics. *J. Chem. Phys.* **139**:025102 (12p.).
21. Zusman L.D. (1994) Dynamic solvent effects in electron transfer reactions. *Z. Phys. Chem.* **186**:1–29.
22. Bixon M., Jortner J. (1999) Electron transfer – from isolated molecules to biomolecules. *Adv. Chem. Phys*. **106**:35–202.

Received September, 2019